

Perfluoropentacene: High-Performance p–n Junctions and Complementary Circuits with Pentacene

Youichi Sakamoto,[†] Toshiyasu Suzuki,^{*,†} Masafumi Kobayashi,[‡] Yuan Gao,[‡] Yasushi Fukai,[‡]
Youji Inoue,[§] Fumio Sato,[§] and Shizuo Tokito[§]

Institute for Molecular Science, Myodaiji, Okazaki 444-8787, Japan, New Products Development Division, Kanto Denka Kogyo Co., Ltd., 1-2-1 Marunouchi, Chiyoda-ku, Tokyo 100-0005, Japan, and NHK Science and Technical Research Laboratories, Kinuta, Setagaya-ku, Tokyo 157-8510, Japan

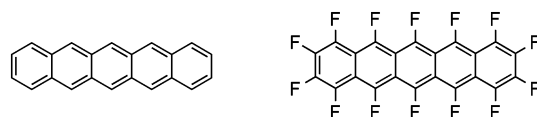
Received April 24, 2004; E-mail: toshy@ims.ac.jp

Organic field-effect transistors (OFETs) are of great interest because of applications for plastic electronics such as electronic papers and flexible displays.¹ Pentacene (C₂₂H₁₄) is a planar aromatic hydrocarbon (Chart 1) and has been widely studied as a p-type semiconductor for OFETs. Of all the OFET materials reported so far, the highest field-effect mobility has been recorded in pentacene (0.3–0.7 cm² V⁻¹ s⁻¹ on SiO₂/Si substrates,² 1.5 cm² V⁻¹ s⁻¹ on chemically modified SiO₂/Si substrates,³ and 3 cm² V⁻¹ s⁻¹ on polymer gate dielectrics⁴). When one considers producing bipolar transistors^{5,6} and complementary circuits^{7,8} with pentacene, the n-type organic semiconductor should have similar physical and electrical properties except for the type of carriers. Previously, we demonstrated that aromatic perfluorocarbons such as perfluoro-*p*-sexiphenyl (C₃₆F₂₆) were efficient n-type semiconductors for the electron-transport layer of organic light-emitting diodes.⁹ Because fluorine is the most electronegative of all the elements and relatively small (hydrogen < fluorine < carbon), perfluorination is an effective way to convert a p-type organic semiconductor to an n-type one without changing the molecular size greatly. We have designed perfluoropentacene (C₂₂F₁₄) as a potential n-type semiconductor for OFETs (Chart 1). Perfluoropentacene is expected to be a planar and crystalline material with high electron affinity. We report herein the synthesis, characterization, and X-ray structure of perfluoropentacene.^{10,11} OFETs with this perfluorocarbon have been fabricated, and bipolar OFETs and complementary circuits with pentacene are also presented.

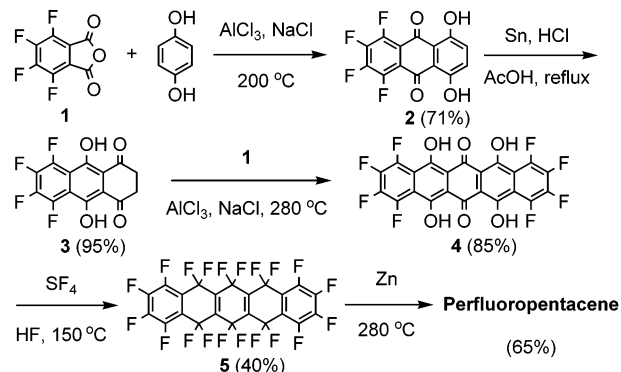
Perfluoropentacene has been synthesized as shown in Scheme 1. The Friedel–Crafts reaction of tetrafluorophthalic anhydride (**1**) with hydroquinone in the presence of aluminum chloride and sodium chloride at 200 °C gave anthraquinone **2** in 71% yield.¹² Reduction of **2** with tin yielded 2,3-dihydro-1,4-anthracenedione **3** in 95%.¹² Again, the Friedel–Crafts reaction of **1** with **3** at 280 °C provided 6,13-pentacenedione **4** in 85% yield. Fluorination of **4** with sulfur tetrafluoride in hydrogen fluoride^{10b} at 150 °C afforded perfluoro-(5,6,7,12,13,14-hexahdropentacene) (**5**) in 40% yield. Defluorination of **5** with zinc^{10b} at 280 °C gave perfluoropentacene in 65% yield.

Perfluoropentacene was purified by train sublimation¹³ and used for characterization. It is a dark blue crystalline solid and slightly soluble in hot 1,2-dichlorobenzene. Its structure was determined by mass spectrometry, elemental analysis, and X-ray crystallography.¹⁴ The UV–vis absorption spectra of pentacene and perfluoropentacene were measured in 1,2-dichlorobenzene. Both acenes show five major peaks in the range of 400 to 700 nm, but their shapes are quite different.¹⁴ The HOMO–LUMO gaps obtained

Chart 1. Structures of Pentacene and Perfluoropentacene



Scheme 1. Synthesis of Perfluoropentacene



from the onset of absorption are 2.07 eV for pentacene and 1.95 eV for perfluoropentacene. The emission maxima in 1,2-dichlorobenzene exhibit a red shift from pentacene (589 nm) to perfluoropentacene (652 nm).¹⁴

The electrochemical measurements on pentacene and perfluoropentacene were performed in 1,2-dichlorobenzene. The differential pulse voltammogram (DPV) of pentacene shows a reduction peak at –1.87 V and an oxidation peak at 0.22 V (versus the ferrocene/ferrocenium couple). As expected, the reduction and oxidation peaks of perfluoropentacene (–1.13 and 0.79 V, respectively) shift positively relative to pentacene.¹⁴ The reduction potential of perfluoropentacene is almost the same as that of C₆₀ (–1.14 V by DPV under the same conditions), which is known as an excellent n-type semiconductor for FETs.¹⁵ The HOMO–LUMO gaps obtained from the redox peaks are 2.09 eV for pentacene and 1.92 eV for perfluoropentacene. Density functional theory (DFT) calculations are in agreement with the experimental results: The HOMO–LUMO gaps calculated at the B3LYP/6-31G(d) level are 2.21 eV for pentacene and 2.02 eV for perfluoropentacene.¹⁴

Single crystals of perfluoropentacene were successfully grown by slow sublimation at 260 °C under a flow of 250 Pa of argon. A dark blue plate was used for X-ray crystallography.¹⁶ The structure of perfluoropentacene is planar as observed for pentacene (Figure 1). The C–C bond distances range from 1.35–1.45 Å and are quite similar to those of pentacene (1.34–1.46 Å).¹⁷ The C–F bond distances (1.34–1.35 Å) are typical of aromatic organofluorine compounds. As shown in Figures 2a and 2b, pentacene and perfluoropentacene adopt herringbone structures with the angles

[†] Institute for Molecular Science.

[‡] Kanto Denka Kogyo Co., Ltd.

[§] NHK Science and Technical Research Laboratories.

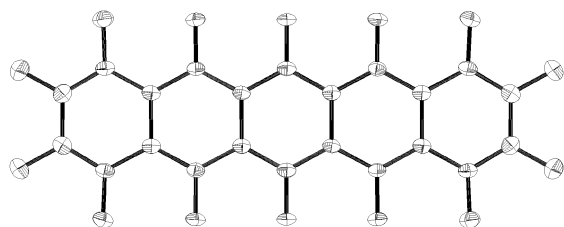


Figure 1. ORTEP drawing of the molecular structure of perfluoropentacene.

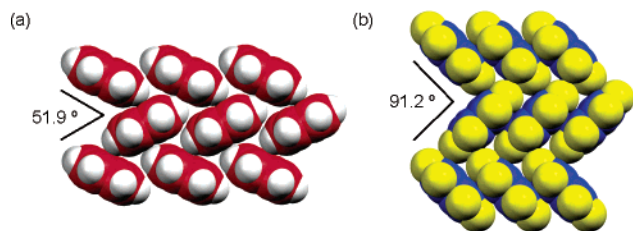


Figure 2. Molecular packing diagrams of (a) pentacene (ref 17) and (b) perfluoropentacene.

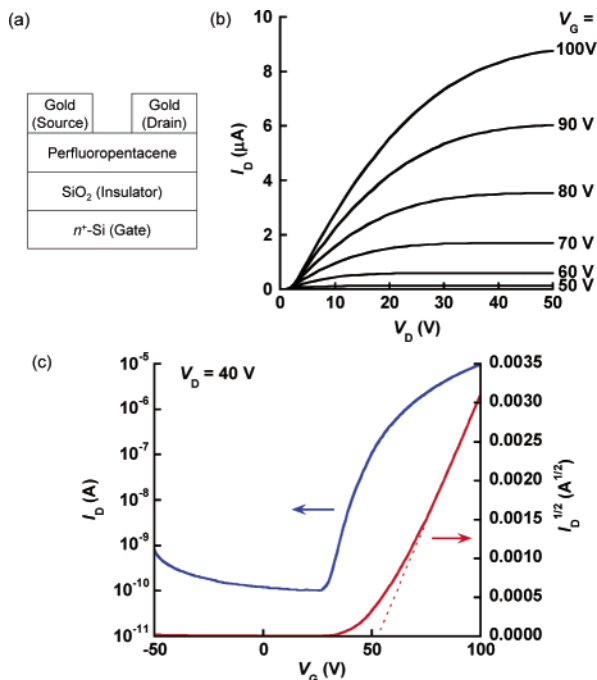


Figure 3. (a) Structure of a perfluoropentacene OFET. (b) Drain current (I_D) versus drain voltage (V_D) characteristics as a function of gate voltage (V_G) for a perfluoropentacene OFET on OTS-modified SiO₂ ($T_{\text{sub}} = 50$ °C). (c) I_D and $I_D^{1/2}$ versus V_G plots at $V_D = 40$ V for the same device. The field-effect mobility calculated in the saturation regime is $0.11 \text{ cm}^2 \text{ V}^{-1} \text{ s}^{-1}$.

of 51.9 and 91.2°, respectively. In pentacene, the intermolecular C–C contacts are longer than 3.64 Å. Interestingly, short C–C contacts (3.22–3.25 Å) less than the sum of van der Waals radii (3.40 Å) were observed in perfluoropentacene.¹⁴ The interplanar distance within the stack is 3.21 Å, which is shorter than the layer separation of graphite (3.35 Å). This is probably because of the electrostatic interaction between electropositive pentacene moieties and electronegative fluorine atoms.

OFETs with perfluoropentacene were constructed on SiO₂/Si substrates using top-contact geometry (Figure 3a).¹⁴ The gate is an n-type Si wafer, and the gate insulator is a 200 nm thick layer of thermally grown SiO₂. The thin film of perfluoropentacene (35 nm) was formed on SiO₂ by high-vacuum evaporation (5×10^{-5} Pa) at different substrate temperatures. Gold source and drain contacts

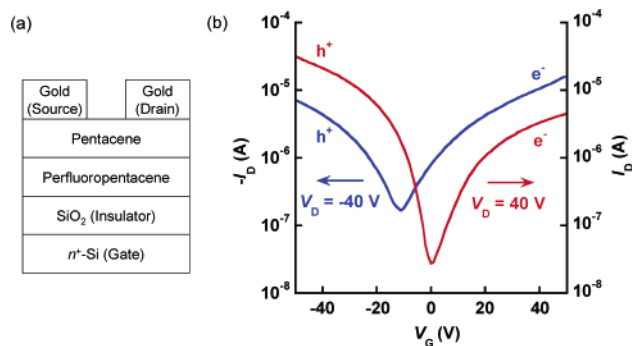


Figure 4. (a) Structure of a perfluoropentacene/pentacene bipolar OFET. (b) Drain current (I_D) versus gate voltage (V_G) characteristics at drain voltages $V_D = -40$ and 40 V for a perfluoropentacene/pentacene bipolar OFET. The field-effect mobilities are calculated to be 0.024 and 0.035 $\text{cm}^2 \text{ V}^{-1} \text{ s}^{-1}$ for the n- and p-channel operations, respectively.

(50 nm) were deposited on the organic layer through a shadow mask. The channel length (L) and width (W) are 100 and 1000 μm , respectively. The electrical measurements for the devices were carried out at room temperature in a vacuum chamber (10^{-5} Pa) without exposure to air. The n-channel FET activity was observed at the substrate temperatures between 25 and 60 °C. The electron mobilities calculated in the saturation regime range from 0.043 to 0.049 $\text{cm}^2 \text{ V}^{-1} \text{ s}^{-1}$, and the on/off ratios are 10^4 – 10^5 . The FET performances are improved when SiO₂ is treated with octadecyltrichlorosilane (OTS). Figure 3b shows the drain current (I_D) versus drain voltage (V_D) characteristics for a perfluoropentacene OFET on an OTS–SiO₂/Si substrate at various gate voltages (V_G). Figure 3c indicates the I_D and $I_D^{1/2}$ versus V_G plots at $V_D = 40$ V for the same device. The highest mobility of 0.11 $\text{cm}^2 \text{ V}^{-1} \text{ s}^{-1}$ was observed at $T_{\text{sub}} = 50$ °C (on/off ratio = 10^5). For comparison, a pentacene OFET with the same channel length and width was fabricated on OTS–SiO₂ at $T_{\text{sub}} = 50$ °C. The hole mobility is 0.45 $\text{cm}^2 \text{ V}^{-1} \text{ s}^{-1}$, and the on/off ratio is 10^6 . Because the electron mobility of perfluoropentacene is comparable to the hole mobility of pentacene, perfluoropentacene is a good candidate for bipolar OFETs and complementary circuits with pentacene. Although *N,N'*-dioctyl-3,4,9,10-perylene tetracarboxylic diimide recorded the highest electron mobility of all the n-channel materials (0.6 $\text{cm}^2 \text{ V}^{-1} \text{ s}^{-1}$),¹⁸ its bipolar OFETs and complementary circuits have not been reported.

Bipolar OFETs with pentacene and perfluoropentacene were fabricated using top-contact geometry (Figure 4a). Perfluoropentacene (10 nm) was evaporated on an OTS–SiO₂/Si substrate at $T_{\text{sub}} = 50$ °C. Then, the second layer of pentacene (35 nm) was formed on the perfluoropentacene layer at the same substrate temperature. Gold source and drain contacts (50 nm) were deposited on the pentacene layer through a shadow mask ($L = 75 \mu\text{m}$; $W = 1000 \mu\text{m}$). The drain current versus gate voltage characteristics (Figure 4b) indicate that the OFET functions at both negative and positive gate voltages with rather narrow off regions ($V_G = 0$ V for $V_D = 40$ V and $V_G = -11$ V for $V_D = -40$ V). When the gate is biased positively relative to the off region, the device works as a normal n-type perfluoropentacene OFET. The field-effect mobility is calculated to be 0.024 $\text{cm}^2 \text{ V}^{-1} \text{ s}^{-1}$ for the n-channel operation. When the gate is biased negatively relative to the off region, an accumulation layer of holes is formed in the pentacene layer, not in the perfluoropentacene layer. In this case, the device functions as a p-type pentacene OFET. The field-effect mobility is 0.035 $\text{cm}^2 \text{ V}^{-1} \text{ s}^{-1}$ for the p-channel operation. When perfluoropentacene is deposited on the first layer of pentacene, the device also works well as a bipolar OFET.¹⁴ The field-effect mobilities for the p- and

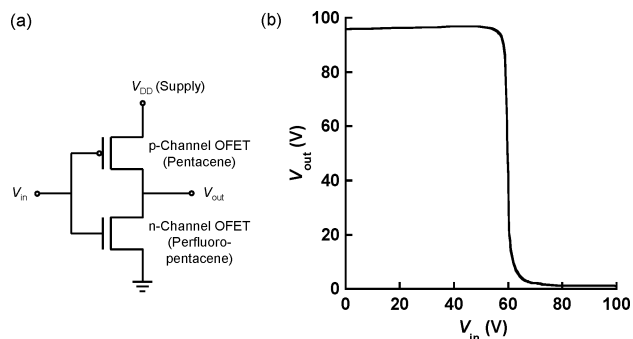


Figure 5. (a) Inverter circuit configuration. (b) Transfer characteristics of a pentacene/perfluoropentacene complementary inverter with a 100 V supply.

n-channel operations are 0.52 and $0.022 \text{ cm}^2 \text{ V}^{-1} \text{ s}^{-1}$, respectively.

Thin films of perfluoropentacene were deposited on OTS-SiO₂/Si substrates by vacuum evaporation at different substrate temperatures ($T_{\text{sub}} = 25, 50, \text{ and } 70 \text{ }^\circ\text{C}$). The X-ray diffraction at room temperature shows reflections up to the third order.¹⁴ The d -spacing calculated from the first reflection peak is 15.8 \AA , which is close to the d -spacing observed in the single crystal (15.5 \AA). In the case of pentacene, the d -spacing of the thin-film phase (15.4 \AA)¹⁹ is much larger than that of the single crystal (14.1 \AA).¹⁷

Pentacene and perfluoropentacene have similar molecular shapes and sizes, and their thin-film d -spacings are almost identical (15.4 and 15.8 \AA , respectively). This may lead to the continuous crystal growth at the interface as if a single material is used.¹⁴ The well-ordered second layer can be formed, and good electrical contacts between the two layers are expected. The stacking interactions are generally found in cocrystals of aromatic and perfluoroaromatic compounds such as benzene and perfluorobenzene.²⁰ There should be such an interaction between pentacene and perfluoropentacene at the interface, which could be another reason for the improved p-n junction. The first bipolar OFET consisted of α -sexithiophene (p-type) and C₆₀ (n-type).⁵ These compounds have completely different d -spacings, which causes inferior quality of the second layer. Ambipolar transport in OFETs with a single organic semiconductor has been reported, but the mobilities were less than $10^{-4} \text{ cm}^2 \text{ V}^{-1} \text{ s}^{-1}$ for both channel types.²¹

A p-channel pentacene OFET ($L = 200 \text{ }\mu\text{m}$; $W = 1000 \text{ }\mu\text{m}$) and an n-channel perfluoropentacene OFET ($L = 100 \text{ }\mu\text{m}$; $W = 1000 \text{ }\mu\text{m}$) were constructed on the same OTS-SiO₂/Si substrate using shadow masks. These OFETs were connected in an inverter circuit configuration (Figure 5a). The transfer characteristics with a 100 V supply exhibit a sharp inversion of the output signal with a high voltage gain of 57 (Figure 5b). Organic complementary circuits reported previously showed lower gains, probably because of low electron mobilities of n-type semiconductors such as copper hexadecafluorophthalocyanine.^{8,22}

In conclusion, perfluoropentacene is the n-type organic semiconductor of choice for constructing high-performance p-n junctions and complementary circuits with pentacene. Organic integrated circuits²³ based on pentacene/perfluoropentacene complementary inverters would exhibit higher operating frequencies. For the solution-processed OFETs, the synthesis of soluble perfluoropen-

tacene precursors is possible by adaptation of the procedures for soluble pentacene precursors.^{24,25} The p-n junctions between aromatic and perfluoroaromatic compounds may be useful for other applications such as organic photovoltaic cells.²⁶

Acknowledgment. This work was supported by Japan Society for the Promotion of Science (Grant-in-Aid for Scientific Research B14340226 and Grant-in-Aid for Young Scientists B15750161). We thank Prof. H. Kawaguchi and Dr. T. Matsuo for help in X-ray structural determination.

Supporting Information Available: Experimental details, absorption and emission spectra, DPVs, DFT calculations, molecular packing diagrams, I_D versus V_G characteristics for a pentacene/perfluoropentacene bipolar OFET, and X-ray diffractograms (PDF); X-ray crystallographic data in CIF format. This material is available free of charge via the Internet at <http://pubs.acs.org>.

References

- (1) Dimitrakopoulos, C. D.; Malenfant, P. R. L. *Adv. Mater.* **2002**, *14*, 99–117.
- (2) Gundlach, D. J.; Lin, Y.-Y.; Jackson, T. N.; Nelson, S. F.; Schlom, D. G. *IEEE Electron Device Lett.* **1997**, *18*, 87–89.
- (3) Lin, Y.-Y.; Gundlach, D. J.; Nelson, S. F.; Jackson, T. N. *IEEE Electron Device Lett.* **1997**, *18*, 606–608.
- (4) Klauk, H.; Halik, M.; Zschieschang, U.; Schmid, G.; Radlik, W.; Weber, W. *J. Appl. Phys.* **2002**, *92*, 5259–5263.
- (5) Dodabalapur, A.; Katz, H. E.; Torsi, L.; Haddon, R. C. *Science* **1995**, *269*, 1560–1562.
- (6) Dodabalapur, A.; Katz, H. E.; Torsi, L.; Haddon, R. C. *Appl. Phys. Lett.* **1996**, *68*, 1108–1110.
- (7) Dodabalapur, A.; Laquindanum, J.; Katz, H. E.; Bao, Z. *Appl. Phys. Lett.* **1996**, *69*, 4227–4229.
- (8) Lin, Y.-Y.; Dodabalapur, A.; Sarpeshkar, R.; Bao, Z.; Li, W.; Baldwin, K.; Raju, V. R.; Katz, H. E. *Appl. Phys. Lett.* **1999**, *74*, 2714–2716.
- (9) Heidenhain, S. B.; Sakamoto, Y.; Suzuki, T.; Miura, A.; Fujikawa, H.; Mori, T.; Tokito, S.; Taga, Y. *J. Am. Chem. Soc.* **2000**, *122*, 10240–10241.
- (10) Perfluoroanthracene (C₁₄F₁₀): (a) Harrison, D.; Stacey, M.; Stephens, R.; Tatlow, J. C. *Tetrahedron* **1963**, *19*, 1893–1901. (b) Oksenko, B. G.; Shteingarts, V. D.; Yakobson, G. G. *Zh. Org. Khim.* **1971**, *7*, 745–751.
- (11) Synthesis of perfluorotetracene (C₁₈F₁₂) was also successful and will be reported elsewhere.
- (12) Kim, S. H.; Matsuoka, M.; Yodoshi, T.; Kitao, T. *Chem. Express* **1986**, *1*, 129–132.
- (13) Wagner, H. J.; Loutfy, R. O.; Hsiao, C.-K. *J. Mater. Sci.* **1982**, *17*, 2781–2791.
- (14) See Supporting Information for the experimental details.
- (15) Haddon, R. C.; Perel, A. S.; Morris, R. C.; Palstra, T. T. M.; Hebard, A. F.; Fleming, R. M. *Appl. Phys. Lett.* **1995**, *67*, 121–123.
- (16) Crystal data for perfluoropentacene: monoclinic, space group $P2_1/c$, $a = 15.51(1) \text{ \AA}$, $b = 4.490(4) \text{ \AA}$, $c = 11.449(11) \text{ \AA}$, $\beta = 91.567(13)^\circ$, $V = 797.0(13) \text{ \AA}^3$, $T = 173 \text{ K}$, $Z = 2$, $R = 0.064$, $\text{GOF} = 1.02$.
- (17) Matheus, C. C.; Dros, A. B.; Baas, J.; Meetsma, A.; de Boer, J. L.; Palstra, T. T. M. *Acta Crystallogr.* **2001**, *C57*, 939–941.
- (18) Malenfant, P. R. L.; Dimitrakopoulos, C. D.; Gelorme, J. D.; Kosbar, L. L.; Graham, T. O.; Curioni, A.; Andreoni, W. *Appl. Phys. Lett.* **2002**, *80*, 2517–2519.
- (19) Dimitrakopoulos, C. D.; Brown, A. R.; Pomp, A. *J. Appl. Phys.* **1996**, *80*, 2501–2508.
- (20) Meyer, E. A.; Castellano, R. K.; Diederich, F. *Angew. Chem., Int. Ed.* **2003**, *42*, 1210–1250.
- (21) Chesterfield, R. J.; Newman, C. R.; Pappenfus, T. M.; Ewbank, P. C.; Haukaas, M. H.; Mann, K. R.; Miller, L. L.; Frisbie, C. D. *Adv. Mater.* **2003**, *15*, 1278–1282.
- (22) Lefenfeld, M.; Blanchet, G.; Rogers, J. A. *Adv. Mater.* **2003**, *15*, 1188–1191.
- (23) Crone, B.; Dodabalapur, A.; Lin, Y.-Y.; Filas, R. W.; Bao, Z.; LaDuca, A.; Sarpeshkar, R.; Katz, H. E.; Li, W. *Nature* **2000**, *403*, 521–523.
- (24) Herwig, P. T.; Müllen, K. *Adv. Mater.* **1999**, *11*, 480–483.
- (25) Afzali, A.; Dimitrakopoulos, C. D.; Breen, T. L. *J. Am. Chem. Soc.* **2002**, *124*, 8812–8813.
- (26) Peumans, P.; Uchida, S.; Forrest, S. R. *Nature* **2003**, *425*, 158–162.

JA0476258